A New Approach on the Egyptian Black Sand Ilmenite Alteration Processes

Mohamed Ismail Moustafa

Nuclear Materials Authority, Egypt

ismail2251962@yahoo.com

ABSTRACT

Several studies have investigated the process of alteration of ilmenite, especially in black sand. To predict the mechanisms of ilmenite alteration and the role of some minor element oxides in the alteration process, separated non-magnetic altered ilmenite grains were examined using a binocular microscope and a Cameca SX-100 microprobe instrument. Twenty intergrown phases of alteration products were concluded in three postulated scenarios for the following alteration processes, carried out after forming the most stable lowest Leached pseudorutile (LPSR) phase $FeTi_3O_6(OH)_3$. Most of the alteration phases of pseudorutile (PSR) and LPSR have real Ti/(Ti+Fe) ratios between 0.6 and 0.75. Some misleading calculations of definite analyzed ilmenite alteration spots showed that all the analyzed TiO_2 percentage is contained within the chemical formula of the analyzed LPSR phase. In these cases, the false Ti/(Ti+Fe) ratios attain up to 0.9, the false included total number of anions (O, OH) ranges between 7 and 8.5, and the associated molecular water ranged between half and two water molecules (0.5-2 H_2O). In these cases, the structure of the remaining LPSR phase may be intergrown with a separated individual triple rutile phase, which appears to have the same X-Ray Diffraction (XRD) pattern as the single PSR phase, or intergrown with a cryptocrystalline TiO_2 phase. Some molecular formulas of PSR or Hydroxylian PSR (HPSR) from previous studies were discussed and explained following the proposed approach.

Keywords-Egypt; black sand; altered ilmenite; leached pseudorutile; hydroxylian pseudorutile

I. INTRODUCTION

Several studies have investigated the alteration products of ilmenite, and various definitions have been proposed for leucoxene. Identification of the intermediate altered compound pseudorutile (PSR) was difficult in earlier studies due to its appearance in fine grain size (30°A), its poor crystallinity, and the similarity of most of its diffraction lines with those of other phases [1]. Thus, it is safe to say that the distinct isotropic phase, previously called arizonite, amorphous iron titanate, and pro-arizonite, was PSR [2-4]. The name PSR was proposed for the product of oxidation and progressive partial removal of iron due to the alteration of ilmenite that produces an intermediate iron titanate of a definite structure [5]. Ilmenite can be altered under reducing conditions [6-7]. The change from ilmenite to PSR involves a phase change in the oxide structure [8]. According to [9], the alteration of ilmenite to PSR decreases cell volume by up to 13%, while it is 6% and reaches 40% by alteration to leucoxene, leading to shrinkage cracks [10]. There are more extensive nanopore networks in the Hydroxylian PSR (HPSR) than in PSR [11]. The detrital ilmenite grains of heavy mineral sands in Brazil are sometimes extremely altered in PSR, anatase (grain boundaries), and leucoxene [12]. There are two types of detrital ilmenite alteration. Type I is an alteration sequence of ilmenite-hydrated ilmenite-PSR-leucoxene, and in Type II, ilmenite is directly altered to HPSR [10]. Type II alteration involves dissolution-reprecipitation [10, 13] or dissolution-hydration [11].

PSR is an intermediate alteration product that commonly occurs in the early stages of alteration (weathering or early diagenesis under weakly reducing conditions) and alters to leucoxene during continued diagenesis [14]. Leucoxene is as conductive as rutile but more magnetic, as rutile is nonmagnetic [15]. Several types of magnetic and non-magnetic altered ilmenite varieties were detected in [16], which explained the formation of each of these altered varieties. The alteration process of Egyptian beach ilmenite was investigated in [17-20]. The chemical composition of highly altered leucoxenated Egyptian beach ilmenite grains was examined using a scanning electron microscope, showing that TiO_2 ranged between 59.45 and 89.72 wt%, the total iron content (Fe_2O_3) ranged from 2.34 to 32.68 wt%, and the SiO_2 content ranged from 0.89 to 8.19 wt% [21]. In some leucoxenated grains, residual particles of ilmenite were enclosed in many of the altered ilmenite grains and some grains were still preserved with the crystal form of the parent ilmenite [22].

Most of the mineralogical features and textures of an obtained high-grade ilmenite concentrate were investigated in [23-24]. According to [25-26], altered ilmenite grains have a wide range of magnetic mass susceptibilities. They can be separated as magnetic at a wide range of 0.1 and 1 A. The highly altered leucoxenated grains (secondary rutile) are separated as nonmagnetic at 1 A. The altered ilmenite grains, which are separated as magnetic at 0.5 and 1 A, contain an enrichment of altered silicate minerals, silica, sphene, and

individual phases of Ti and Fe as oxyhydroxides and TiO_2. In addition, relatively higher contents of structural water are detected in the molecular formulas of the investigated LPSR phases, in addition to considerable volumes of voids and cracks. These are the reasons for the relatively lower magnetic characteristics of these grains. However, leucoxene may be defined as a partially or completely altered ilmenite having a wide range of chemical compositions, which embarrass the recorded crystal structure and may not represent all the included alteration phases. Some or all altered phases may be amorphous, crypto- or micro-crystalline, or have an identical X-Ray Diffraction (XRD) pattern. This study investigated the altered ilmenite grains obtained as nonmagnetic at 1 A. Several Excel spreadsheets were formulated to conclude the chemical formulas of the various ilmenite alteration products. Based on the investigation and interpretation of the various data obtained, a new approach was proposed for the mechanisms of the ilmenite alteration processes. Furthermore, the conclusions of some previous studies are re-explained, and their unknown extending chemical formulas are well-defined and given.

II. MATERIAL AND METHODS.

A large bulk sample of naturally highly concentrated beach black sand was collected from the Abu Khashaba beach area on the Mediterranean coast, 7 km east of Rosetta estuary. The sample represents the raw sand in a 4 km stretch with variable widths, from a few to 20 meters. The sand was manually scraped from the mantle to a depth ranging from 10-30 cm. This study investigated altered ilmenite grains obtained as a nonmagnetic fraction at 1 A. Most grains were very close to the relatively heavier magnetically altered ilmenite grains obtained at 1 A [25] but had relatively lighter colors. Using the difference in physical characteristics between the various economic minerals [16, 23-25], the collected surface naturally highly concentrated beach raw sand was processed using the following equipment and processes:

- Reading cross-belts magnetic separator to differentiate the raw sample into three fractions: a ferromagnetic, a bulk magnetic, and a bulk non-magnetic.

- Full-size Wilfley shaking tables for wet-gravity concentration of the bulk nonmagnetic fraction obtained.

- Carpco HP 167 high-tension roll-type electrostatic separator to treat the concentrate to obtain a bulk rutile conductor fraction and a bulk zircon nonconductor fraction.

- Carpco MIH 13-231-100 industrial high-intensity induced roll dry magnetic separator to separate the bulk rutile conductor fraction obtained.

- Frantz isodynamic magnetic separator: The three successive magnetic fractions obtained from the last treatment stage were mixed as a bulk magnetic fraction, composed of hematite, ilmeno-hematite, different varieties of magnetic primary rutile, and various grades of altered ilmenite grains, in addition to minor Cr-bearing and other magnetic minerals [16]. A relatively smaller representative sample of the bulk magnetic fraction was obtained and subjected to magnetic differentiation using the Frantz isodynamic magnetic separator with the following adjusted operating conditions: longitudinal slope of 20°, side slope of 5°, feeding rate of 30 g/hour, and six different successive currents: 0.1, 0.2, 0.25. 0.35, 0.5, and 1 A. Six magnetic and one nonmagnetic fractions were obtained. This study investigated the altered ilmenite grains obtained in the individual nonmagnetic fraction separated at 1 A.

- Microscopic investigation: The altered ilmenite grains obtained from the separated individual nonmagnetic fraction was investigated using binocular and reflected microscopes.

- Microprobe analysis: The different altered ilmenite grains were examined in a Cameca SX-100 Electron Micro Probe Analyzer (EMPA), at the Institute of Mineralogy and Crystal Chemistry, Stuttgart University, Germany, equipped with three Wavelength Dispersive Spectrometers (WDS) and an Energy Dispersive Spectrometer (EDS). The whole surface of the polished sections was examined by Backscattered Electron (BSE) images so that grains with 10 µm size or even smaller obtained could be detected. The analytical conditions were: 15 kV accelerating voltage, 15 nA electron current, 180s counting time for each spot analyzed in the investigated grains, and a focused electron beam diameter of 1 to 4 µm. The following standards were used: diopside for Mg and Ca, albite for Na, corundum for Al, orthoclase for Si and K, rutile for Ti, rhodonite for Mn, Fe_2O_3 for Fe, Cr_2O_3 for Cr, V for V, and sphalerite for Zn. $K\alpha$ lines were used for each element analyzed. From the obtained nonmagnetic fraction, a definite number of grains were picked and polished for investigation using the microprobe.

- Philips PW 3710/31 XRD with automatic sample changer PW 1775, 21 positions, using a scintillation counter, Cu-target tube, Ni filter at 40 kV and 30 mA, connected to a computer using an X-40 diffraction program and ASTM cards for mineral identification.

All Excel spreadsheets used for the calculation of different molecular formulas of mineral phases, which is the final result of the essence and calculation algorithms, are available upon request [25, 26].

III. RESULTS

Six grains were investigated in the nonmagnetic fraction at 1 A. They were secondary rutile with TiO_2, Fe_2O_3, and total oxide sum ranging between 89.05-99.86 wt%, 0.03-8.8 wt%, and 94.55-100.76 wt%, respectively. Their chemical composition ranged from ferriferous rutile and rutile with a considerable amount of molecular and/or structural water. An amazing altered leucoxene grain was detected during the investigation of some secondary rutile grains of grayish-white colors in the nonmagnetic fraction at 1 A, as shown in Figure 1 and Table I. In this grain, the TiO_2 content increased from 77.06 wt% in spot 1 to 90.78 wt% in spot 18, while the Fe_2O_3 content decreased from 5.37 wt% to 3.24 wt%, respectively. The increase in TiO_2 was 13.7 wt% while the corresponding decrease in Fe_2O_3 was 2.2 wt%. The decrease in Fe_2O_3 from spot 1 to spot 18 was very low and not negatively correlated with the relatively higher increase rate of TiO_2. The Fe_2O_3

content does not have a definite tendency to increase or decrease through all the various spots analyzed in the grain, as shown in Table I. It is difficult to believe that the enrichment of TiO_2 content is due to such decreasing Fe_2O_3 content values. The identification for most economic minerals of the Egyptian black sand and other sand deposits using the XRD technique were explained in [16, 27]. The non magnetic altered ilmenite

grains at 1 A, were subjected to the XRD before and after roasting at 1100 °C for 1 hr. Before roasting, the XRD pattern of the grains was composed of only rutile but its diffraction lines were diffused indicating that it is of bad crystalline structure. After roasting, the XRD pattern of the sample gave the well defined pattern of rutile.

TABLE I.   THE MICROPROBE CHEMICAL ANALYSES AND CORRESPONDING MOLECULAR FORMULAE OF THE ANALYZED SPOTS OF THE ALTERED GRAYISH-WHITE GRAIN OF FIGURE 1, SEPARATED AS NONMAGNETIC AT 1 A

Spot	SiO₂	MgO	MnO	CaO	ZnO	Fe₂O₃	Al₂O₃	Cr₂O₃	Na₂O	K₂O	TiO₂	O Total	OH%	H₂O%	N Total	Fe₂	Ti₃	Ox	OHy	Lost Fe	Ti/(Ti+Fe)
1	0.66	0.07	0.06	0.19	0.00	5.37	0.61	0.19	0.08	0.07	77.06	84.36	27.89	14.77	99.13	0.32	3	3.95	5.05	1.68	0.90
2	0.70	0.07	0.00	0.19	0.00	5.29	0.58	0.18	0.24	0.19	77.11	84.54	27.81	14.73	99.27	0.34	3	3.96	5.04	1.66	0.90
3	0.74	0.09	0.04	0.32	0.00	4.68	0.55	0.12	0.33	0.16	78.07	85.10	28.22	14.95	100.05	0.32	3	3.90	5.10	1.68	0.90
4	0.69	0.07	0.01	0.05	0.00	2.94	0.25	0.04	0.03	0.05	79.18	83.32	30.77	16.30	99.61	0.18	3	3.55	5.45	1.82	0.94
5	0.60	0.07	0.01	0.29	0.00	4.83	0.58	0.17	0.12	0.06	83.53	90.27	28.87	15.29	105.56	0.28	3	3.81	5.19	1.72	0.92
6	0.57	0.06	0.03	0.21	0.00	4.58	0.61	0.16	0.09	0.04	84.42	90.75	29.24	15.49	106.23	0.26	3	3.76	5.24	1.74	0.92
7	0.61	0.07	0.02	0.23	0.00	3.73	0.46	0.17	0.04	0.03	85.77	91.12	30.10	15.94	107.06	0.21	3	3.64	5.36	1.79	0.93
8	0.60	0.08	0.00	0.19	0.00	3.95	0.54	0.17	0.03	0.04	84.27	89.85	29.81	15.79	105.64	0.22	3	3.68	5.32	1.78	0.93
9	0.67	0.07	0.00	0.19	0.00	4.34	0.55	0.23	0.07	0.07	85.04	91.22	29.36	15.55	106.77	0.25	3	3.74	5.26	1.75	0.92
10	0.55	0.03	0.00	0.15	0.00	3.61	0.53	0.17	0.02	0.02	85.59	90.66	30.30	16.05	106.71	0.20	3	3.61	5.39	1.80	0.94
11	0.66	0.04	0.01	0.19	0.00	4.00	0.55	0.20	0.03	0.02	86.36	92.05	29.81	15.79	107.84	0.22	3	3.68	5.32	1.78	0.93
12	1.11	0.18	0.00	0.07	0.00	4.99	0.56	0.06	0.03	0.05	86.01	93.06	28.57	15.13	108.19	0.28	3	3.86	5.14	1.72	0.91
13	0.17	0.02	0.00	0.06	0.00	4.73	0.34	0.12	0.04	0.04	87.74	93.24	30.28	16.04	109.28	0.20	3	3.60	5.40	1.80	0.94
14	0.22	0.07	0.01	0.07	0.00	4.97	0.34	0.09	0.11	0.03	87.86	93.77	29.96	15.87	109.63	0.22	3	3.64	5.36	1.78	0.93
15	0.29	0.03	0.00	0.13	0.00	4.47	0.36	0.09	0.08	0.10	88.02	93.57	30.22	16.01	109.58	0.21	3	3.61	5.39	1.79	0.93
16	0.16	0.03	0.01	0.03	0.00	4.09	0.06	0.04	0.01	0.03	89.12	93.56	31.22	16.53	110.09	0.15	3	3.46	5.54	1.85	0.95
17	0.51	0.04	0.03	0.11	0.00	3.39	0.35	0.07	0.05	0.02	90.59	95.16	30.98	16.41	111.57	0.17	3	3.51	5.49	1.83	0.95
18	0.10	0.01	0.00	0.05	0.00	3.24	0.09	0.03	0.04	0.02	90.78	94.36	31.94	16.92	111.28	0.12	3	3.37	5.63	1.88	0.96
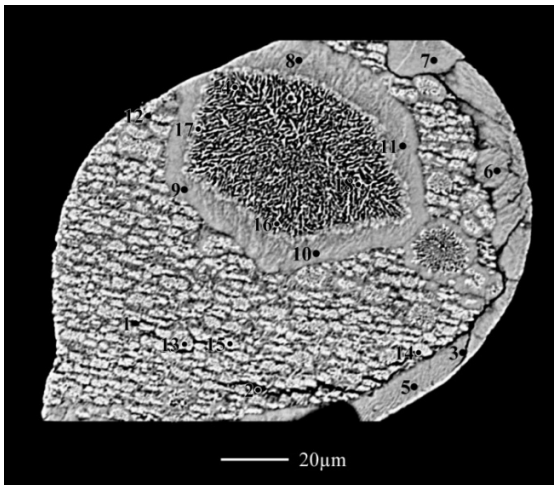
Fig. 1.   BSE image and chemical analysis spots of the altered-grayish white ilmenite grain, separated as non-magnetic at 1 A.

IV.   DISCUSSION

The original total oxide sum (OT) was equal to 84.36 wt% in spot 1, 95.16 wt% in spot 17, and 94.4 wt % in spot 18. The OT of spot 18 is 10 wt% and 10.8 wt% greater than that in spots 1 and 17, respectively. The increase in OT in these spots essentially varies directly with the increase in TiO_2 content, while the differences in the other oxides analyzed are very low. Therefore, the enrichment of TiO_2 content for the different spots is most probably due to a loss of appreciable contents of structural and/or molecular water. After applying the PSR Excel spreadsheet, the first four spots (Figure 1, spots 1-4) appear to be LPSR, according to the results of Table I. In these

four spots, the new calculated total sum of the analyzed oxides (NT) ranged between 99.13 and 100.05 wt%, and the cationic iron content ranged between 0.18 and 0.34. Therefore, it is difficult for each of them to be a PSR, as it is mainly composed of an individual phase of TiO_2 in addition to the minor content of Fe_2O_3. Some spots contain mixed individual phases for TiO_2 and Fe_2O_3 and seem falsely LPSR. The investigation of the BSE image of the grain reflects its composition of several similar units. Each unit is composed of various dark-light or black-white zones that may reflect differences in structural and/or molecular water content. These detected zones include black zones, gray zones, white zones, and mixed grayish-white zones. These zones also seem to be different in their content of TiO_2, in addition to their content of structural and/or molecular water.

Investigating the relatively larger unit on the upper left of the grain showed that it was a combination of several small units that comprise the whole grain and in which the structural and/or molecular water begins to be removed. The relatively smaller unit at the lower right of the grain, which also attaches to the relatively larger unit at the upper left, is an indication of the aforementioned explanation. It seems that in each of these units of the detected grain, the contained structural water begins to differentiate between the various detected dark-light zones. After that, each similar dark or light zone of the various small units is connected to form one sector area, like that of the relatively larger unit at the upper left of the grain. A careful investigation of the chemical composition of the spots shows that the relatively lighter zones contain a relatively higher TiO_2 content and a relatively lower content of structural and/or molecular water. In the relatively darker zones, the TiO_2 content is relatively lower, while the structural and/or

molecular water content is relatively higher. The detected various dark-light zones of the relatively smaller units are not highly clear as those of the relatively larger unit at the upper left of the detected grain. It can be concluded that, in the white zones, most of the Ti-bearing phase is present mainly as oxide, while in the black zones, it is present mainly as oxyhydroxide. Due to the relatively lower iron content in the various analyzed spots, the presence of Fe^{3+}-bearing phase as oxy, oxyhydroxide, or hydroxide phase does not greatly affect the enrichment of TiO_2 content. Additionally, the spots of the dark black zones analyzed in the outer region of the grain may have the possible characteristic lowest chemical composition of the LPSR formula component $FeTi_3O_6(OH)_3$ during the final stages of alteration.

The tetragonal rutile structure seems to be more compact than the hexagonal PSR structure. Therefore, it does not allow considerable content of OH^- inside it. Hence, the presence of Ti^{4+} and maybe Fe^{3+} as oxyhydroxide or hydroxide phases is not desired in appreciable amounts within the tetragonal rutile structure. In the white zones, the recorded water content seems to be largely molecular rather than structural, and vice versa in the black zones. Table II shows that the dehydroxylation process proceeds gradually with the transition from black zones to gray, grayish-white, and finally white zones. It is clear that there is a definite relation between both the analyzed contents of SiO_2 and Al_2O_3, and perhaps also CaO, and the recorded structural water content. In the grayish-white and white zones, these oxides are highly diminished, as shown in Table II.

TABLE II.   CHEMICAL COMPOSITION OF THE DIFFERENT ANALYZED SPOTS OF THE SEPARATED NON-MAGNETIC GRAIN OF FIGURE 1, SHOWING THE VARIOUS INVESTIGATED COLOURED ZONES AND THEIR CHEMICAL COMPOSITION RANGE CONTENTS OF TiO_2, FE_2O_3 AND STRUCTURAL (STR)/MOLECULAR (MOL) WATER

Spot	Zone Type	TiO₂	Fe₂O₃	SiO₂	Al₂O₃	Cao	Cr₂O₃	MgO	MnO	Na₂O	K₂O	Total	TiO₂ content range	Fe₂O₃ content range	STR & MOL H₂O content range
1	Outer black	77.1	5.4	0.7	0.6	0.19	0.19	0.07	0.06	0.08	0.07	84.4	77.1-78.1	4.7-5.4	15.6-14.9
2		77.1	5.3	0.7	0.6	0.19	0.18	0.07	0.00	0.24	0.19	84.5			
3		78.1	4.7	0.7	0.6	0.32	0.12	0.09	0.04	0.33	0.16	85.1			
4	Inner black	79.2	2.9	0.7	0.3	0.05	0.04	0.07	0.01	0.03	0.05	83.3	79.2	2.9	16.7
5	Outer grey	83.5	4.8	0.6	0.6	0.29	0.17	0.07	0.01	0.12	0.06	90.3	83.5-85.8	3.7-4.8	9.7-8.9
6		84.4	4.6	0.6	0.6	0.21	0.16	0.06	0.03	0.09	0.04	90.8			
7		85.8	3.7	0.6	0.5	0.23	0.17	0.07	0.02	0.04	0.03	91.1			
8	Inner grey	84.3	4.0	0.6	0.5	0.19	0.17	0.08	0.00	0.03	0.04	89.9	84.3-86.4	3.6-4.3	10.1-7.9
9		85.0	4.3	0.7	0.6	0.19	0.23	0.07	0.00	0.07	0.04	91.2			
10		85.6	3.6	0.6	0.5	0.15	0.17	0.03	0.00	0.02	0.02	90.7			
11		86.4	4.0	0.7	0.6	0.19	0.20	0.04	0.01	0.03	0.02	92.1			
12	Outer Greish white	86.0	5.0	1.1	0.6	0.07	0.06	0.18	0.00	0.03	0.05	93.1	86-88	4.5-5	6.9-6.2
13		87.7	4.7	0.2	0.3	0.06	0.12	0.02	0.00	0.04	0.04	93.2			
14		87.9	5.0	0.2	0.3	0.07	0.09	0.07	0.01	0.11	0.03	93.8			
15		88	4.5	0.3	0.4	0.13	0.09	0.03	0.00	0.08	0.10	93.6			
16	Inner white	89.1	4.1	0.2	0.1	0.03	0.04	0.03	0.01	0.01	0.03	93.6	89.1-90.8	3.2-4.1	6.4-4.8
17		90.6	3.4	0.5	0.4	0.11	0.07	0.04	0.03	0.05	0.02	95.2			
18		90.8	3.2	0.1	0.1	0.05	0.03	0.01	0.00	0.04	0.02	94.4			

The presence of more than one iron oxidation state (Fe^{2+}, Fe^{3+}) contained in ilmenite ($FeTiO_3$ or $Fe_3Ti_3O_9$) may be the reason for the alteration into various products. Hence, under definite environmental conditions, ilmenite is unstable due to the oxidation of Fe^{2+} to Fe^{3+} inside its structure, which will be associated with the partial leaching of some iron content and the formation of another unstable phase called leached ilmenite. The leaching of one-third of the ferric iron content produces another mineral phase, called PSR $Fe^{3+}_2Ti_3O_9$, which contains several micro-fissures, cracks, and pores that are formed not only during the leaching stage of ilmenite but possibly also during the various stages of weathering, transportation, deposition, and/or diagenesis in some ilmenite deposits. Additionally, such fissures and cracks may be due to selective alteration processes (e.g. dissolution) under definite environmental conditions for some impurities (inclusions) or exsolved intergrowths of various mineral components occurring in definite parts and orientations for many of the non-homogeneous ilmenite grains. However, the presence of such microstructures of ilmenite grains may increase the activity of molecular water and the chances of oxidation and alteration of ilmenite.

According to [25-26], considering that the chemical formula of ilmenite is $Fe_3Ti_3O_9$, the contents of TiO_2, FeO, and Fe_2O_3 in the leached ilmenite formed range between 51.39-59.19 wt%, 39.84-0.02 wt%, and 3-37.02 wt%, respectively. Fe^{2+} ranged between 0 and 2.46, while Fe^{3+} ranged between 0.17 and 1.94. The Ti/(Ti+Fe) ratio ranged between 0.51 and 0.6, almost the same as [28], which gives ranges between 0.5 and 0.6. The Fe/Ti ratio ranged from 0.91 to 0.67, which is different from the given by [29] that stated that the molar ratio Fe/Ti for ilmenite is 1.02, decreases to approximately 0.84 for pseudo-ilmenite and 0.64 for PSR. NT ranged between 90.24 and 101.27 wt%. Most of the values were much lower than 100 wt%, reflecting the role of molecular water in the process of ilmenite oxidation into leached ilmenite and also the following alteration stages in the PSR and LPSR phases.

According to [30-31], oxidation occurs by water or steam in the absence of air. With the aid of small amounts of HCl (as a catalyst), siderite ($FeCO_3$) is oxidized to $Fe(OH)_3$ at $150°C$, and magnetite becomes Fe_2O_3 at 200°C. These are probably not the minimum temperatures at which these reactions become noticeable. The following two concurrent equations for ilmenite alteration were suggested by [32]:

Anodic oxidation mechanism:

$$3Fe^{2+}_{0.93}Mn^{2+}_{0.07}TiO_3 \rightarrow$$
$$Fe^{3+}_{1.86}Mn^{3+}_{0.14}Ti_3O_9 + 0.93Fe^{3+} + 0.07Mn^{3+} + e^- \quad (1)$$
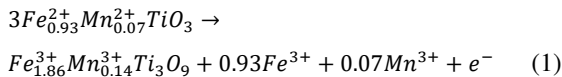
Cathodic half-cell reaction:

$$0.25O_2 + 0.5H_2O + e^- \rightarrow (OH^-) \quad (2)$$
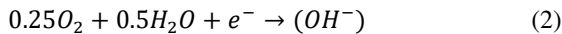
According to them, the formed (OH^-) readily complexes with Fe^{3+} of (1) to form goethite. By neglecting Mn^{2+} in (1) and multiplying (2) in (3), the last two equations can be reformulated as follows:

$$3Fe^{2+}TiO_3 \rightarrow Fe^{3+}_2Ti_3O_9 + Fe^{3+} + 3e^- \quad (3)$$

$$0.75O_2 + 1.5H_2O + 3e^- \rightarrow 3(OH^-) \quad (4)$$
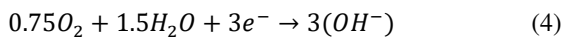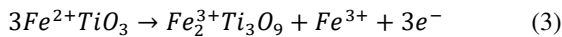
However, by summation of (3) and (4) we get:

$$3Fe^{2+}TiO_3 + 0.75O_2 + 1.5H_2O \rightarrow$$
$$Fe^{3+}_2Ti_3O_9 + Fe^{3+} + 3(OH^-) \quad (5)$$
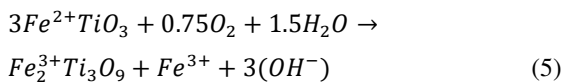
The last equation is the same as the first equation obtained from the model of [33], where both Fe^{3+} and OH^- combine to give $Fe^{3+}(OH)_3$, in addition to the formed PSR ($Fe^{3+}_2Ti_3O_9$). This reaction operates in a saturated, mildly acidic oxygenated water environment below the water table [10, 33]. If the produced $3OH^-$ of (4) is complexed with the ferric iron of PSR $Fe^{3+}_2Ti_3O_9$ and then bonded with it replacing $3O_2^-$ by losing another Fe^{3+}, then:

$$Fe^{3+}_2Ti_3O_9 + 3(OH^-) \rightarrow$$
$$FeTi_3O_6(OH)_3 + Fe^{3+} + 3O_2 \quad (6)$$
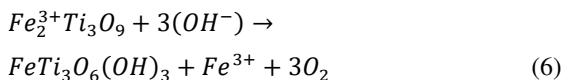
Therefore, by the summation of (3), (4), and (6):

$$3Fe^{2+}TiO_3 + 0.75O_2 + 1.5H_2O \rightarrow$$
$$Fe^{3+}Ti_3O_6(OH)_3 + 2Fe^{3+} + 3O_2 \quad (7)$$
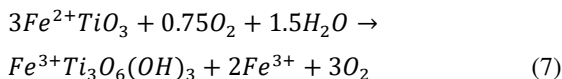
The situation in (7) requires that Fe^{3+} does not form $Fe(OH)_3$ in the products of (5). Hence, hematite is formed instead of $Fe^{3+}(OH)_3$ or goethite. After that, hematite is directly leached or can be changed to goethite and then leached. The exsolved hematite inside the titanhematite-ferriilmenite exsolved intergrown grains of the Egyptian black sand is altered to goethite, which is lost, leaving the titanhematite lamella as empty voids or pits. Meanwhile, most of the ferriilmenite component of the grain remains unchanged. This explanation may be responsible for some recorded Egyptian beach ilmenite varieties known as pitted ilmenite [18], skeletal ilmenite [20, 34], or microporous ilmenite [16]. However, regardless of the occurrence of (6) and (7), the PSR phase obtained from (5) appears to be altered into another PSR phase by losing ferric iron and replacing oxygen with hydroxide. When one Fe^{3+} is lost, three O^{2-} are replaced by three OH^- due to water hydrolysis to achieve the electrical neutralization of the new LPSR phase obtained. The combination of hydration with oxidation causes an increase in water content together with a linear decrease in Fe^{2+} iron content in the composition region from ilmenite to PSR and encompasses hydrated (leached) ilmenite as shown in [11, 35].

The further removal of Fe^{3+} beyond the PSR composition is followed by the breakdown into TiO_2 and Fe_2O_3. This process proceeds through a leaching and reprecipitation mechanism in a mildly reducing acidic solution [33]. According to [36], the model of [33] has several weaknesses. The two model's reactions require different environments to proceed. The first requires an oxidizing one and the second a reducing one, with its reliance on reducing conditions in near-surface conditions. However, within the PSR composition range (60-71% TiO_2), the water content increased from ~2 to 4.5 wt% with decreasing iron oxide content [37], suggesting that the intermediate alteration phases comprised mixtures of TiO_2 with iron hydroxides.

A. The New Approach of Ilmenite Alteration

At the end of the leached ilmenite phase, most of the ferrous iron Fe^{2+} is oxidized into ferric, where one-third of the ilmenite's iron content is removed and another definite chemical formula phase is formed. This new phase is called PSR: $Fe^{3+}_2Ti_3O_9$.

In the obtained PSR formula, the TiO_2 content almost equals 60 wt % and the remaining 40 wt % is mainly for Fe_2O_3 and other associated oxides. The given values of the Ti/(Ti+Fe) ratios for PSR vary across studies: 0.5-0.7 [38], 0.57-0.7 [9], 0.6-0.7 [28], 0.6 [39], 0.6-0.79 or 0.80 [11]. The lower chemical composition formula limit of PSR is $Fe_2Ti_3O_9$ [33], $Fe_{1.5}Ti_3O_{7.5}(OH)_{1.5}$ [28], while [9] considered the average composition of LPSR as $FeTi_3O_6(OH)_3$, and the lower stability limit lies around 0.6 mol% Fe or slightly higher, as related to 3 mol% Ti.

According to [25-26], in the analyzed spots of PSR and LPSR, the contents of TiO_2 and Fe_2O_3 range between 56.76 and 86.56 wt%, and 37.3 and 6.68 wt%, respectively. The Ti/(Ti+Fe) ratio ranges between 0.60-0.88. The PSR and LPSR chemical formulas are as follows: $Fe_{2.01-0.42}Ti_3O_{9-4.23}(OH)_{0-4.77}$. Only eight analyzed spots have cationic iron ranges between 0.28 and 0.38, while 16 analyzed spots have cationic iron ranges between 0.42 and 0.49. Investigating the backscattered electron images of grains with spots that have cationic iron ranges between 0.42 and 0.49 ensures the existence of some survived LPSR in association with the formed rutile. Then, the lowest cationic iron content of the survived LPSR phase is between 0.42-0.5 with a corresponding molecular formula of $Fe_{0.5-0.42}Ti_3O_{4.26-4.5}(OH)_{4.5-4.74}$. In other words, when the iron content decreases below 0.5, the structure of the present LPSR phase begins to collapse. The complete collapse of the LPSR phase structure into an individual TiO_2 phase appears to be at any value within the range of 0.5-0.4 of iron content. The given values of the Ti/(Ti+Fe) ratio for LPSR are different between studies. In [9], it was found between 0.72 and 0.8, and it ranged between 0.79 or 0.8 and 0.9 in [11]. In [10], it was reported that the analyses of HPR, in the same area studied with [11], had a Ti/(Ti+Fe) ratio of 0.8-0.85, representing 3.3 wt%, while those in the range of 0.85-0.9 represented 2.13 wt% of the total analyses performed. According to [25], when the TiO_2 content of the investigated LPSR phase spots reaches values in the region of 68-70 wt%, the mechanism of alteration seems to be changing. The comparison between OT and NT after applying

the constructed PSR spreadsheet shows that the calculated structural water contents of the analyzed spots are incorrect. In other words, not all the analyzed TiO_2 of the spot is contained in the PSR/LPSR phase. There are other individual phases of TiO_2 and/or Fe_2O_3, since the two main oxides contained in the analyzed spot most probably separate from the LPSR phase [25].

Taking into account the PSR phase formula $Fe_2Ti_3O_9$, when losing a definite amount (x) of Fe^{3+} another formula phase is formed. It is called LPSR $FeTi_3O_6$ $(OH)_3$ (8) and contains (9-$3x$)O^{2-} and ($3x$)OH^-. In this LPSR formula, the TiO_2, Fe_2O_3, and structural water contents are equal to 69.17, 23.05, and 7.79 wt%, respectively. It was detected that during the alteration of the PSR phase $Fe_2Ti_3O_9$ to the LPSR phase $FeTi_3O_6(OH)_3$, there is no change in the alteration mechanism. Most of the chemical analyses of the investigated LPSR spots lie within the range of these two chemical formulas, which give acceptable results on applying the constructed PSR-LPSR spreadsheets. The last chemical formula phase, $FeTi_3O_6(OH)_3$, is considered the most stable lowest iron LPSR structure for its content of OH^-. In this LPSR formula, the OH/O ratio is equal to 0.5. Then, each of the three Ti atoms seems to be stable with this ratio of surrounding O and OH. When the number of O anions becomes less than six, their corresponding negative charges become less than 12, e.g., in the LPSR formula $Fe_{0.83}Ti_3O_{5.5}(OH)_{3.5}$, the three Ti atoms seem to become unstable. In this LPSR formula phase, losing a definite amount (x) of Fe^{3+} (for example $x=1/6$ or 0.17 Fe^{3+}), another LPSR formula phase is formed containing (6-$3x$)O and ($3+3x$)OH^-:

$$Fe_{(2-x)}Ti_3O_{(9-3x)}(OH)_{(3x)} = FeTi_3O_6(OH)_3 \quad (8)$$

$$Fe_{(1-x)}Ti_3O_{(6-3x)}(OH)_{(3+3x)} =$$
$$Fe_{0.83}Ti_3O_{5.5}(OH)_{3.5} \quad (9)$$
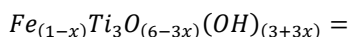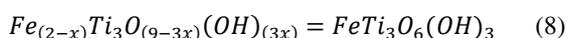
The newly formed LPSR phase starts to rearrange gradually and slowly to maintain its stability. However, according to the lost amount of Fe^{3+} from the LPSR phase $FeTi_3O_6(OH)_3$, several scenarios are expected to occur. The prevailing surrounding environmental conditions affect the deposit, including altered ilmenite grains such as water activity, pH/Eh, and effective time, which can govern the loss rate of Fe^{3+} outside the LPSR structure phase. Therefore, three scenarios are proposed for the lost content of Ti-oxyhydroxide from the LPSR formula structure. Each of them includes several probable cases to achieve the target, as shown in Figures 2-7. On the dehydroxylation of clay minerals, it was stated in [40] that due to greater stiffness, thicker crystallites require more energy to dehydroxylate, which also requires opening of the interlayer [41-42], therefore, there is a need for more thermal energy or higher water pressure provided to rehydroxylate than thinner crystallites. According to [11], there is a more extensive network of nanopores in the HPSR than in the PSR. Then, in the various LPSR alteration scenarios, the alteration processes are gradual and slow and occur on a nano-alteration scale which introduces highly thinner crystallites and facilitates the alteration changes.

1) Scenario A

With the loss of 1/6 Fe^{3+}, then 3×1/6 of oxygen, namely a half O^{2-}, will be replaced by a half OH^- and another LPSR-phase other than $FeTi_3O_6(OH)_3$ will be formed, which is $Fe_{0.83}Ti_3O_{5.5}(OH)_{3.5}$. Figure 2 shows the contents of TiO_2, Fe_2O_3, and structural molecular water in the obtained LPSR phase. However, the obtained LPSR phase structure seems to be relatively less stable and will try to resume the most stable lowest iron LPSR-phase of $FeTi_3O_6(OH)_3$. To achieve the target, four cases may be postulated to occur A1, A2, A3, and A4, as shown in Figure 2. Considering the partial leaching of the altered LPSR $FeTi_3O_6(OH)_3$ of case A1, the content of the separated individual Ti-phase, 1/2(TiO_2) corresponds to three folds of the partially leached LPSR-phase content 1/6($FeTi_3O_6(OH)_3$), and the remaining LPSR phase is 5/6($FeTi_3O_6(OH)_3$). In case A2, the separated individual Ti-phase is TiO_2, which corresponds to three folds the content of the partially leached LPSR-phase content which is 2/6($FeTi_3O_6(OH)_3$), and the remaining LPSR phase is 4/6($FeTi_3O_6(OH)_3$). In case A3, the separated individual Ti-phase is 1.5(TiO_2), which corresponds to three folds the content of the partially leached LPSR-phase content, which is 3/6($FeTi_3O_6(OH)_3$), and the remaining LPSR phase is 3/6($FeTi_3O_6(OH)_3$). In case A4, the separated individual Ti-phase is 2(TiO_2), which corresponds to three folds the content of the partially leached LPSR-phase content, which is 4/6($FeTi_3O_6(OH)_3$), and the remaining LPSR-phase is 2/6($FeTi_3O_6(OH)_3$). In case A1, only a definite amount of Ti-oxyhydroxide will be removed from the LPSR phase, as there is no loss of other additional amounts of Fe^{3+}, as in cases A2, A3, and A4 to adjust the anionic structure of the LPSR obtained. In case A1, the unstable composite alteration phase produced $Fe_{0.83}Ti_3O_6(OH)_{2.5}$, and the false ratio of Ti/(Ti+Fe) is equal to 0.78. If the available surrounding environment conditions are suitable for leaching a relatively higher Fe^{3+} content (e.g., 2/6Fe^{3+}) of the most stable lowest iron LPSR $FeTi_3O_6(OH)_3$, then another expected scenario is formed with another unstable LPSR chemical formula, scenario B.

2) Scenario B

In this scenario, the removed Fe^{3+} content outside the most stable lowest iron LPSR-phase is 2/6Fe^{3+}. Another unstable LPSR chemical formula is obtained $Fe_{0.67}Ti_3O_5(OH)_4$, containing 72.84, 16.21, and 10.75 wt % of TiO_2, Fe_2O_3, and structural molecular water, respectively. This obtained LPSR-phase structure seems to be relatively less stable and will try to resume the most stable lowest iron LPSR $FeTi_3O_6(OH)_3$ phase. To achieve the target, the two cases B1 and B2 of Figure 3 are expected to occur, which can also be obtained by losing 1/6Fe^{3+} from the unstable phase obtained in case A1 $Fe_{0.83}Ti_3O_{5.5}(OH)_{3.5}$. In the B1 and B2 cases, the unstable composite alteration phase produced contains 0.67 cationic iron, and the calculated false ratio of Ti/(Ti+Fe) equals 0.82. When not only Ti-oxyhydroxide is removed but also $Fe(OH)_3$, then another four cases, B3, B4, B5, and B6, of Scenario B are expected to occur, as shown in Figure 4. In all these cases of scenario B, the TiO_2 phase corresponds to three folds of the leached fraction of the original $FeTi_3O_6(OH)_3$. In the two cases B1 and B2, the TiO_2 produced corresponds to 3×2/6($FeTi_3O_6(OH)_3$). In the cases B3 and B4, the 1.5(TiO_2) produced corresponds to 3×3/6($FeTi_3O_6(OH)_3$), while in B5

and B6, the $2(TiO_2)$ produced corresponds to $3 \times 4/6(FeTi_3O_6(OH)_3)$, as shown in Figures 3 and 4.
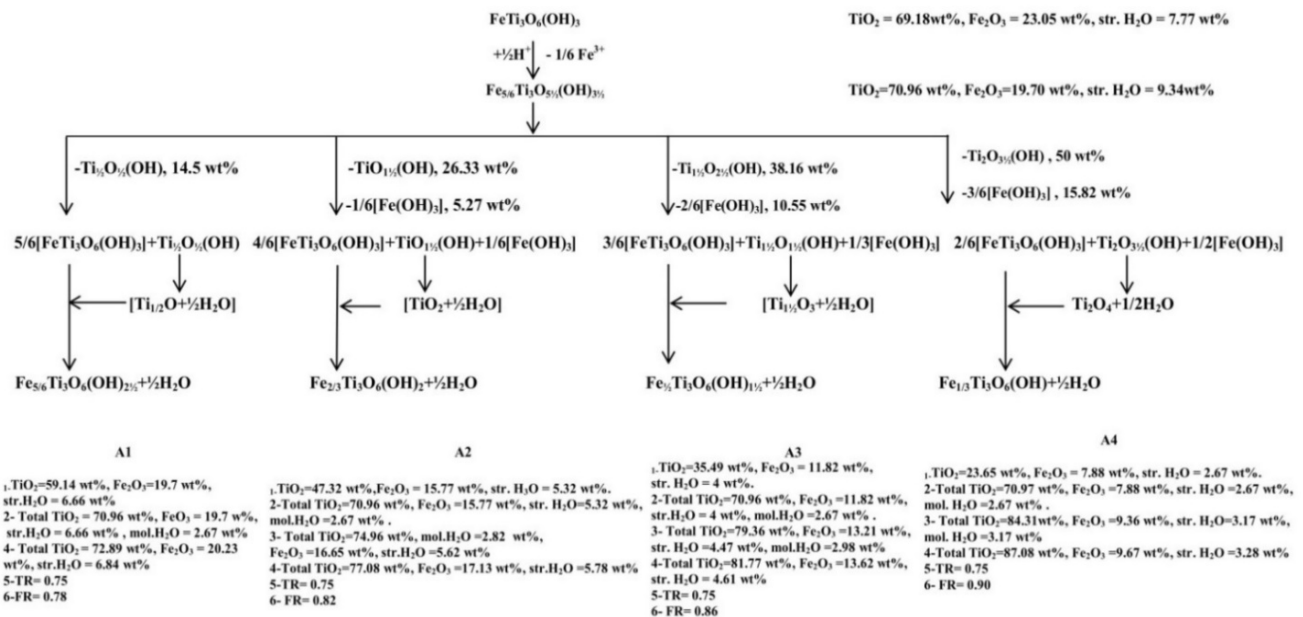
Fig. 2.　　Scenario A including the cases A1, A2, A3, and A4, and their corresponding final products. The label numbers from 1 to 6 in this and the following figures are for the following: 1- The chemical composition of the remaining individual LPSR phase, 2- the mixed chemical composition of the obtained two individual LPSR and titanium dioxide phases, 3- the recalculated mixed chemical composition of the obtained two individual LPSR and titanium dioxide phases after removing only of the produced $Fe(OH)_3$ phase, 4- the recalculated mixed chemical composition of the obtained two individual LPSR and titanium dioxide phases after the removing the produced $Fe(OH)_3$ and mol water, 5- the true (Ti/Ti+Fe) ratio, and 6- the false (Ti/Ti+Fe) ratio.
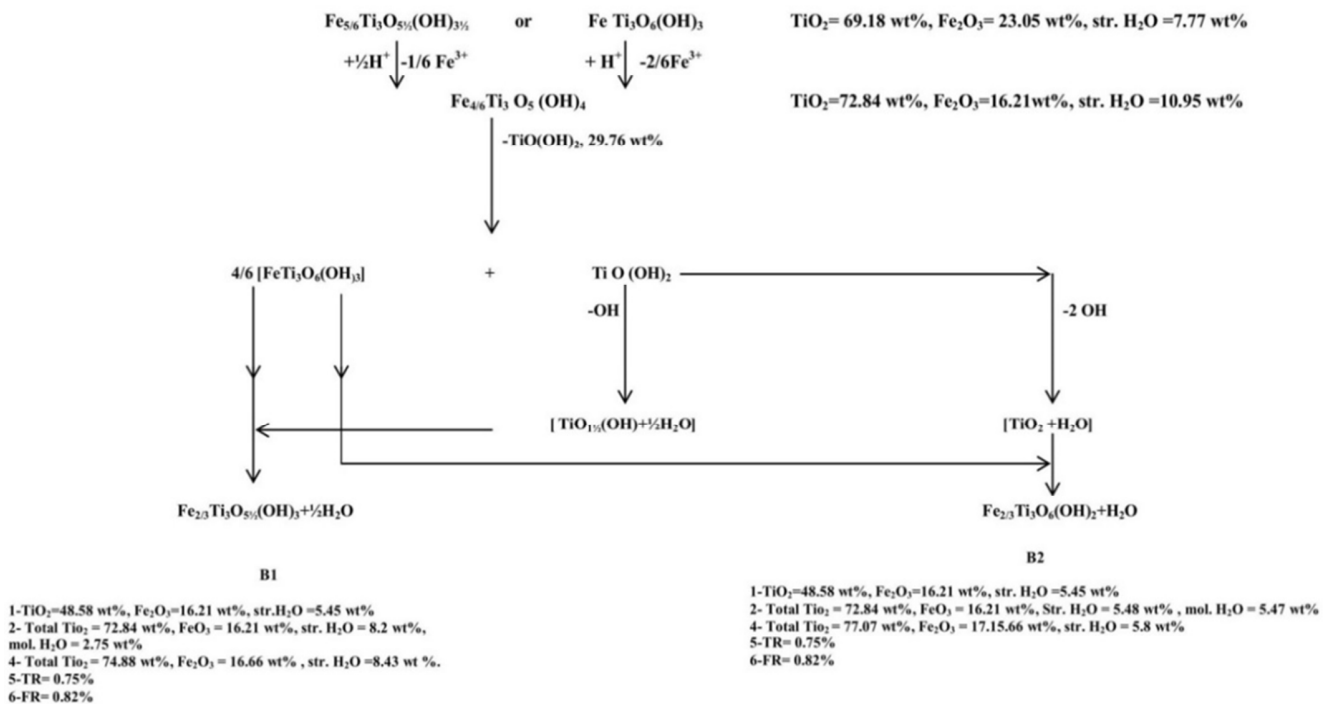
Fig. 3.　　Scenario B including the two probable cases B1 and B2, and their corresponding final products.
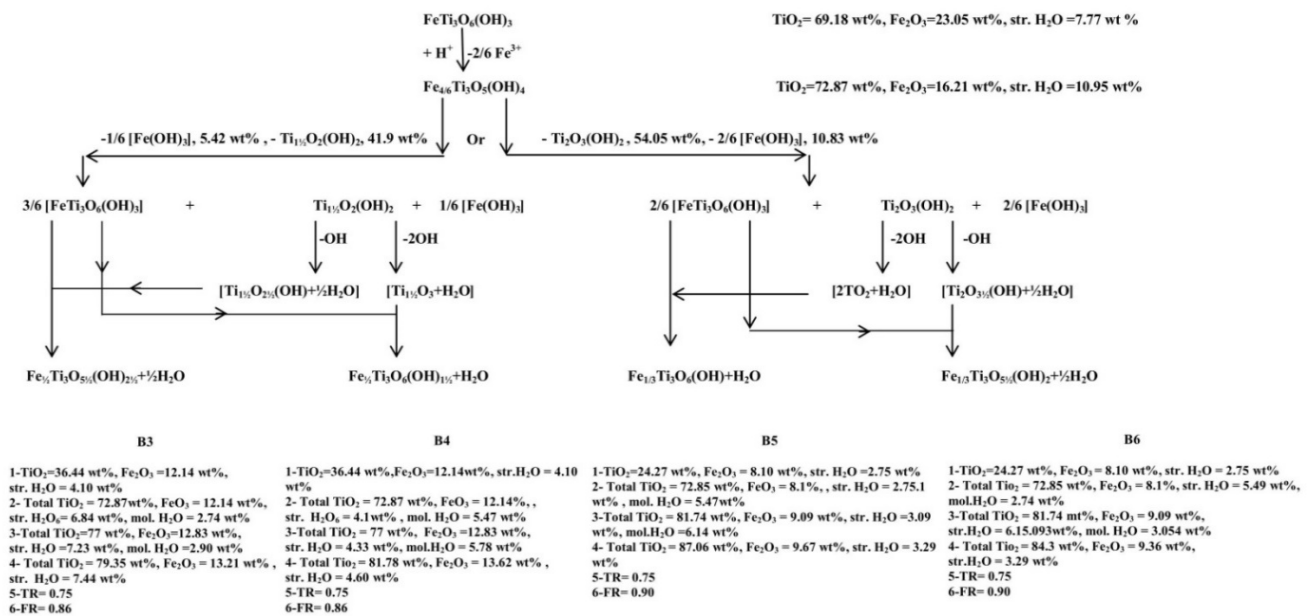
Fig. 4. Scenario B including the other four probable cases B3, B4, B5, and B6, and their corresponding final products.

3) Scenario C

If the Fe^{3+} leached from the most stable LPSR phase is 3/6, then another unstable LPSR chemical formula is obtained $(Fe_{0.5}Ti_3O_{4.5}(OH)_{4.5})$, as shown in Figure 5. The same result can be obtained by losing 1/6 Fe^{3+} from the unstable phase obtained from B1 or B2 $(Fe_{0.67}Ti_3O_5(OH)_4)$. Figure 5 shows the contents of the different components of the new LPSR phase when losing 3/6Fe^{3+}. This LPSR structure appears to be relatively less stable and will try to resume the most stable lowest iron LPSR phase $FeTi_3O_6(OH)_3$. Hence, a definite content of an individual Ti-oxyhydroxide phase will be separated, $Ti_{1.5}O_{1.5}(OH)_3$ and all cases C1, C2, and C3 can be obtained. In these cases, the unstable composite alteration phases produced contain 0.50 cationic iron, and the false ratio of Ti/(Ti+Fe) is 0.86. If the leached Fe^{3+} content outside the most stable LPSR phase is 4/6 instead of 3/6, then another unstable LPSR formula is obtained $(Fe_{2/6}Ti_3O_4(OH)_5)$, as shown in Figure 6. However, the same result can also be obtained by losing 1/6 of Fe^{3+} from the unstable phase obtained from C1, C2, or C3 $(Fe_{3/6}Ti_3O_{4.5}(OH)_{4.5})$. The new LPSR phase in this case has the different component contents shown in Figure 6. The obtained LPSR-phase structure $Fe_{2/6}Ti_3O_4(OH)_5$ appears to be relatively less stable and will try to resume the most stable lowest iron LPSR phase $FeTi_3O_6(OH)_3$. In this case, the separated Ti-oxyhydroxide content must be $Ti_2O_2(OH)_4$, and cases C4, C5, C6, and C7 are expected to occur (Figure 6). In these cases, the unstable composite alteration phases produced contain 0.33 cationic iron and the false ratio of Ti/(Ti+Fe) is 0.90. However, if it was supposed that the separated Ti-oxyhydroxide content is $Ti_2O_{2.5}(OH)_3$, then some iron content, 1/6(Fe (OH)$_3$), must also be removed to obtain finally mixed products composed of the relatively most stable lowest iron LPSR phase $FeTi_3O_6(OH)_3$, in addition to a separated individual TiO_2 or Ti-oxyhydroxide phase in a ratio of 1:3. Then, another three cases, C8, C9, and C10, of scenario C are expected to occur, as shown

in Figure 7. In all 10 cases of scenario C, the TiO_2 produced corresponds to three folds the leached fraction of the original $FeTi_3O_6(OH)_3$ shown in Figures 5-7. Investigating the 20 individual mineralogical phases from the three suggested scenarios gives the data shown in Table III, where True Ratio (TR) is the ratio corresponding only to both Ti and Fe contents in the actual remaining LPSR component phase. The False Ratio (FR) corresponds to the total contents of Ti and Fe of all the contained phases as a final product, in all LPSR and Ti-oxide or Ti-oxyhydroxide individual phases. That is, all of the analyzed TiO_2 wt% of the detected spot is considered. Table IV shows the weight percentages of the various chemical components of the final composite products obtained for the 20 cases of the three scenarios, after removing $Fe(OH)_3$ produced with or without the associated molecular water.

Investigating Tables III and IV shows that some of the final products obtained in the different cases are similar, where only the associated individual molecular water is different. The 20 phases obtained can be reduced to only 10 alteration phases. The 10 cases that will be considered are the A1 case of Scenario A, B1-B2 cases of Scenario B, and C1-C7 cases of Scenario C. In these chosen 10 cases, only unstable immobile titanium oxyhydroxide is separated from the LPSR phase and there is no change in the iron content. It is difficult to accept that other definite amounts of $Fe(OH)_3$ can be separated in association with the separated amount of Ti-oxyhydroxide (cases A2-A4, B3-B6, and C8-C10). In the 10 chosen cases, the TR ratios were 0.75, which is the same as the most stable lowest iron LPSR phase $FeTi_3O_6(OH)_3$, while the FR ratios are different, as shown in Tables III and IV since they range from 0.78 to 0.90. The values of the Ti/(Ti+Fe) ratios for leucoxene vary between studies. This ratio ranged between 0.7-0.9 [38] and 0.7-1 [28]. The Fe/Ti ratio of the given HPSR was 0.33 [39], which corresponds to $FeTi_3O_6(OH)_3$. On the other hand, in [11], it was stated that HPSR had a sum of (O+OH) equal to

7.5 or 8. Therefore, the ratio (O+OH)/Ti in this HPSR was 2.5-2.67, not 3, as in $Fe_2Ti_3O_9$ or $FeTi_3O_6(OH)_3$.

One of the most amazing results is the C2 and C3 cases of scenario C. Multiplying each of the two final products obtained, including also the separated molecular water in (2), the following two chemical formulas are obtained, respectively:

$$(Fe_{0.5}Ti_3O_{5.5}(OH)_{2.5} + H_2O) \times 2$$

$$= FeTi_6O_{11}(OH)_5 + 2H_2O \qquad (10)$$

$$(Fe_{0.5}Ti_3O_6(OH)_{1.5} + 1.5H_2O) \times 2$$

$$= FeTi_6O_{12}(OH)_3 + 3H_2O \qquad (11)$$
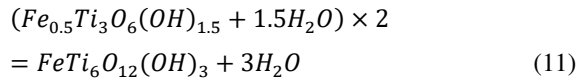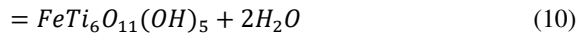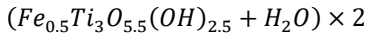
Each of these two formulas is similar to one of the two suggested formulas of HPR given in [11].
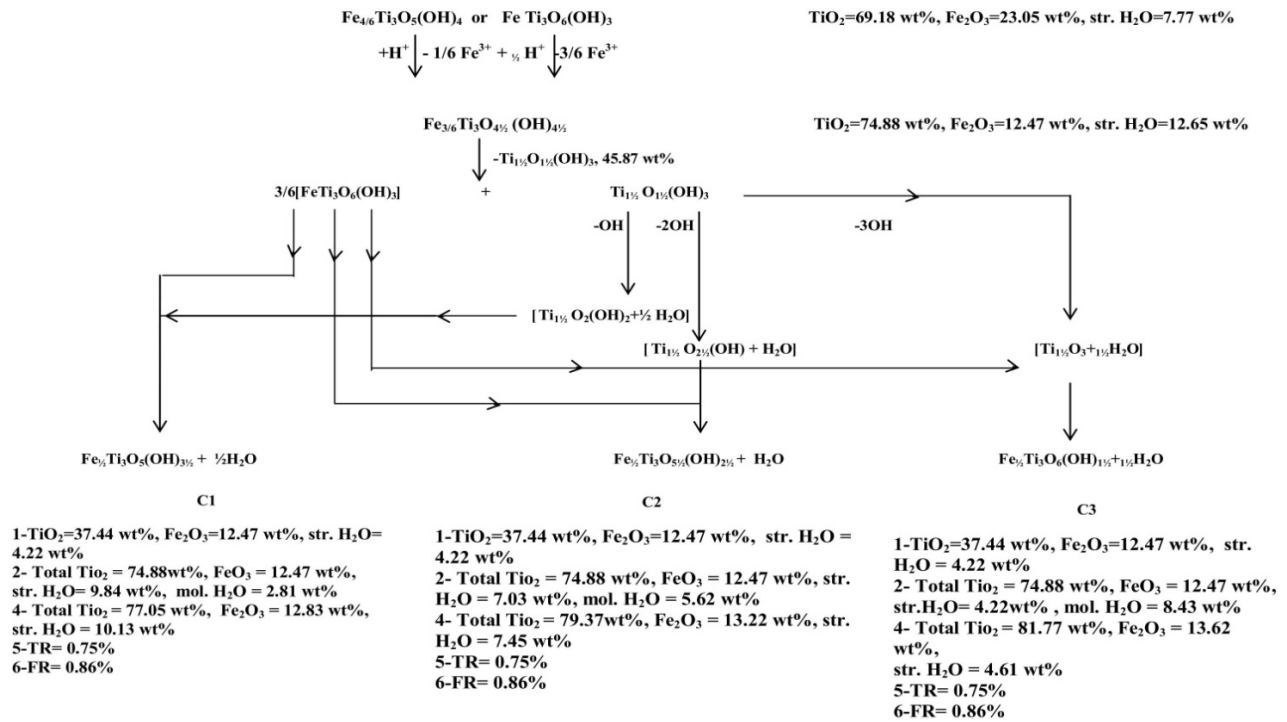
Fig. 5.   Scenario C including the three probable cases C1, C2, and C3, and their corresponding final products.
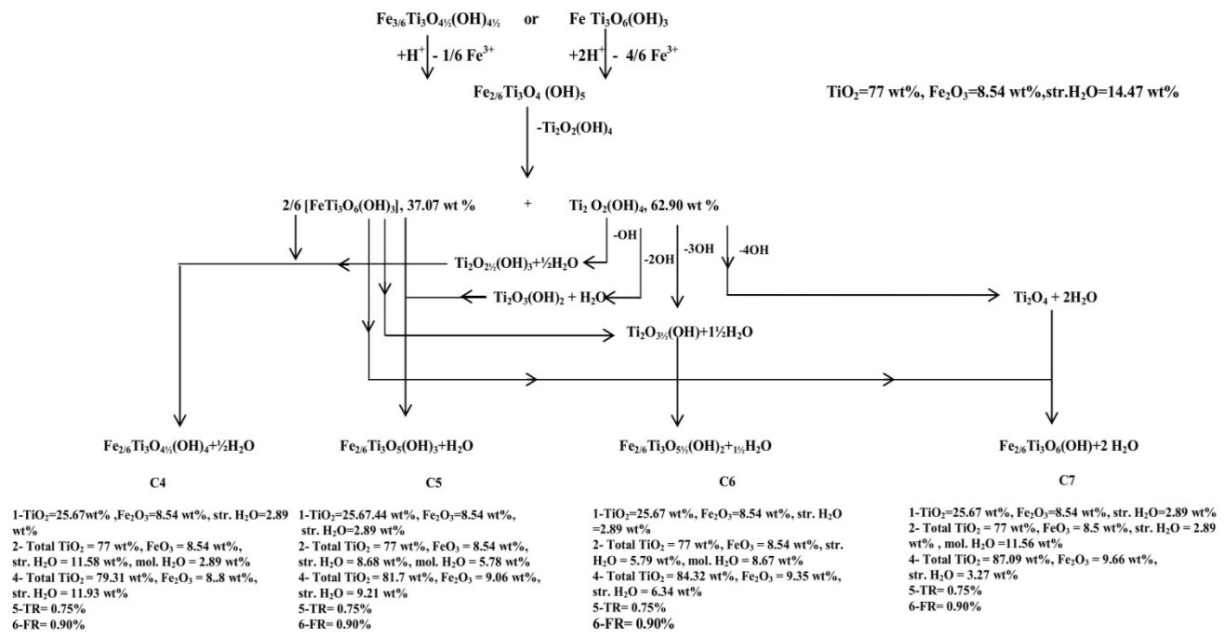
Fig. 6.   Scenario C including the four probable cases C4, C5, C6, and C7, and their corresponding final products.

$FeTi_3O_6(OH)_3$ TiO_2=69.18 wt%, Fe_2O_3=23.05 wt%, str. H_2O=7.77wt%

+1½H^+ -3/6 Fe^{3+}

$Fe_{3/6}Ti_3O_{4½}(OH)_{4½}$ TiO_2=74.88 wt%, Fe_2O_3=12.47 wt%, str. H_2O=12.67wt%

-$Ti_2O_{2½}(OH)_3$, 58.35wt%

- 1/6 [Fe(OH)₃,5.56 wt%

2/6[$FeTi_3O_6(OH)_3$]   + $Ti_2O_{2½}(OH)_3$ +   1/6 $Fe(OH)_3$

-OH -2OH   -3OH

[$Ti_2O_3(OH)_2$ + ½H_2O]

[$Ti_2O_{3½}(OH)$+H_2O]

[2TiO_2 +1½H_2O]

$Fe_{1/3}Ti_3O_5(OH)_3$+½H_2O $Fe_{1/3}Ti_3O_{5½}(OH)_2$+H_2O $Fe_{1/3}Ti_3O_6(OH)$+1½H_2O

C8   **C9**   **C10**

1-TiO_2=24.96 wt%, Fe_2O_3=8.31wt%, str. H_2O = 2.82 wt%
2- Total TiO_2 = 74.88 wt%, Fe_2O_3 = 8.31 wt%, str. H_2O = 8.44 wt%, mol. H_2O = 2.81 wt%
3- Total TiO_2 = 79.20 wt%, Fe_2O_3 = 8.80 wt%, str. H_2O = 8.93 wt%, mol. H_2O = 2.98 wt%
4- Total TiO_2 = 81.70 wt%, Fe_2O_3 = 9.08 wt% , str. H_2O = 9.21 wt%
5-TR= 0.75%
6-FR= 0.90%

1-TiO_2=24.96 wt%, Fe_2O_3=8.31 wt%, str. H_2O = 2.82 wt%
2- Total TiO_2 = 74.88 wt%, Fe_2O_3 = 8.31 wt%, str. H_2O = 5.63 wt%, mol. H_2O = 5.62 wt%
3- Total TiO_2 = 79.30 wt%, Fe_2O_3 = 8.80 wt%, str. H_2O = 5.96 wt%, mol. H_2O = 5.95 wt%
4- Total TiO_2 = 84.31 wt%, Fe_2O_3 = 9.35 wt%, str. H_2O = 6.34 wt%
5-TR= 0.75%
6-FR= 0.90%

1-TiO_2=24.96 wt%, Fe_2O_3=8.31 wt%, str. H_2O =2.82 wt%
2- Total TiO_2= 74.88 wt%, FeO_3= 8.31 wt%, , str. H_2O = 2.82.44 wt%, mol. H_2O = 8.43 wt%
3- Total TiO_2 = 79.30 wt%, Fe_2O_3 = 8.8 wt%, , str. H_2O = 3 wt% , mol. H_2O = 8.9 wt%
4- Total TiO_2 = 87.09 wt%, Fe_2O_3 = 9.67 wt%, str. H_2O = 3.28 wt%
5-TR= 0.75%
6-FR= 0.90%

Fig. 7.   Scenario C including the three probable cases C8,C9, and C10, and their corresponding final products.

TABLE III.   INDIVIDUAL MINERALOGICAL PHASES PRODUCED FROM EACH DIFFERENT SCENARIO PHASE CASE, THEIR CORRESPONDING ANION CONTENTS, MOLECULAR WATER, AND BOTH OF TRUE/FALSE TI/(TI+FE) RATIOS

Scenario cases	The final product of the mixed individual phases	Molecular water content	Number of O^{2-} anions for composite mineral phases	Number of OH^- anions for composite mineral phases	Total number of anions; Σ O, OH	Ti/(Ti+Fe)	
						True	False
A1	5/6[$FeTi_3O_6(OH)_3$], 0.5TiO_2	0.5 H_2O	6 O	2.5OH	8.5	0.75	0.78
A2	4/6[$FeTi_3O_6(OH)_3$],TiO_2	0.5 H_2O	6 O	2OH	8	0.75	0.82
A3	3/6[$FeTi_3O_6(OH)_3$],1.5 TiO_2	0.5 H_2O	6 O	1.5OH	7.5	0.75	0.86
A4	2/6[$FeTi_3O_6(OH)_3$], 2TiO_2	0.5 H_2O	6 O	1 OH	7	0.75	0.90
B1	4/6[$FeTi_3O_6(OH)_3$], $TiO_{1.5}(OH)$	0.5 H_2O	5.5 O	3 OH	8.5	0.75	0.82
B2	4/6[$FeTi_3O_6(OH)_3$], TiO_2	H_2O	6 O	2 OH	8	0.75	0.82
B3	3/6[$FeTi_3O_6(OH)_3$], $Ti_{1.5}O_{2.5}(OH)$	0.5 H_2O	5.5 O	2.5 OH	8	0.75	0.86
B4	3/6[$FeTi_3O_6(OH)_3$], 1.5TiO_2	H_2O	6 O	1.5 OH	7.5	0.75	0.86
B5	2/6[$FeTi_3O_6(OH)_3$], 2TiO_2	H_2O	6 O	1 OH	7	0.75	0.90
B6	2/6[$FeTi_3O_6(OH)_3$], $Ti_2O_{3.5}(OH)$	0.5 H_2O	5.5 O	2 OH	7.5	0.75	0.90
C1	3/6[$FeTi_3O_6(OH)_3$], $Ti_{1.5}O_2(OH)_2$	0.5 H_2O	5 O	3.5 OH	8.5	0.75	0.86
C2	3/6[$FeTi_3O_6(OH)_3$], $Ti_{1.5}O_{2.5}(OH)$	H_2O	5.5 O	2.5 OH	8	0.75	0.86
C3	3/6[$FeTi_3O_6(OH)_3$], 1.5TiO_2	1.5 H_2O	6 O	1.5 OH	7.5	0.75	0.86
C4	2/6[$FeTi_3O_6(OH)_3$], $Ti_2O_{2.5}(OH)_3$	0.5 H_2O	4.5 O	4 OH	8.5	0.75	0.90
C5	2/6[$FeTi_3O_6(OH)_3$], $Ti_2O_3(OH)_2$	H_2O	5 O	3 OH	8	0.75	0.90
C6	2/6[$FeTi_3O_6(OH)_3$], $Ti_2O_{3.5}(OH)$	1.5 H_2O	5.5 O	2 OH	7.5	0.75	0.90
C7	2/6[$FeTi_3O_6(OH)_3$], 2TiO_2	2 H_2O	6 O	1 OH	7	0.75	0.90
C8	2/6[$FeTi_3O_6(OH)_3$], $Ti_2O_3(OH)_2$	0.5 H_2O	5 O	3 OH	8	0.75	0.90
C9	2/6[$FeTi_3O_6(OH)_3$], $Ti_2O_{3.5}(OH)$	H_2O	5.5 O	2 OH	7.5	0.75	0.90
C10	2/6[$FeTi_3O_6(OH)_3$], 2TiO_2	1.5 H_2O	6 O	1 OH	7	0.75	0.90

However, each of the two formulas of cases C2 and C3 of Scenario C is considered to be composed of the relatively most stable lowest iron LPSR phase $FeTi_3O_6(OH)_3$, in addition to the separated individual TiO_2 or Ti-oxyhydroxide phase in a ratio equal to 1:3, respectively, and the presence of one or 1.5 of individual molecular water molecules. Based on chemical and structural analyses of individual HPSR grains, in [11], a composition range was calculated for HPR between approximately $Fe^{3+}Ti_6O_{12}(OH)_3.3H_2O$ and $Fe^{3+}Ti_6O_{11}(OH)_5.2H_2O$, reporting that the full extent of the composition range is unknown and the molecular water is nonstructural, probably absorbed on the surfaces of nanoscale domains of the mineral and associated with impurities in micropores (as H_2O and/or OH). Dividing the two formulas

given in [11] by 2, the composition will range between $Fe_{0.5}Ti_3O_6(OH)_{1.5}.1.5H_2O$ and $Fe_{0.5}Ti_3O_{5.5}(OH)_{2.5}.H_2O$, respectively.

These two chemical formulas do not correspond to the PSR structure despite the XRD patterns of the PSR for the studied HPSR grains obtained. The anionic lattice structure is not the same as the well-defined PSR $Fe_2Ti_3O_9$ or $Fe_{2-n}Ti_3(O_{9-3n},OH_{3n})$, where O+OH=9. It appears that these two formulas of [11] are mixtures between a survivable LPSR and an amorphous TiO_2 phase or the most probably epitaxial growth of the triple rutile

on the hexagonal-packed anion layers of a collapsed part of a preexisting LPSR. Therefore, such an individual TiO_2 phase is either structureless or has the same PSR structure as HPSR. The disappearance of the micro- or crypto-crystalline TiO_2-phase in the XRD pattern of the detected HPR grains of [11] does not mean the absence of an additional individual TiO_2 phase with the HPR structure. The presence of individual TiO_2 content in HPR grains of [11] explains why some HPSR grains were obtained in the non-magnetic fraction at 11 kilogauss, although their grain sizes are +125 μ, like the majority of the magnetic HPR grains.

TABLE IV.   WEIGHT PERCENTAGES OF THE CHEMICAL COMPONENTS FOR THE FINAL COMPOSITE CHEMICAL PRODUCTS OF ALL CASES OF THE THREE PROPOSED SCENARIOS WITH AND WITHOUT THE ASSOCIATED INDIVIDUAL MOLECULAR WATER

Scenario cases	The final obtained composite chemical product	Range of TiO_2 content wt %	Range of Fe_2O_3 content wt %	Range of structural water content wt %	Range of molecular water content wt %
A1	$Fe_{5/6}Ti_3O_6(OH)_{2.5} + 0.5H_2O$	70.96-72.89	19.7-20.23	6.66-6.84	2.67—0
A2	$Fe_{2/3}Ti_3O_6(OH)_2 + 0.5H_2O$	74.96-77.08	16.66-17.13	5.62-5.78	2.82-0
A3	$Fe_{1/2}Ti_3O_6(OH)_{1.5} + H_2O$	79.36-81.77	13.21-13.62	4.47-4.61	2.98-0
A4	$Fe_{1/3}Ti_3O_6(OH) + 0.5H_2O$	84.31-87.08	9.3-9.67	3.17-3.28	3.17-0
B1	$Fe_{2/3}Ti_3O_{5.5}(OH)_3 + 0.5H_2O$	72.84-74.88	16.21-16.66	8.2-8.43	2.75-0
B2	$Fe_{2/3}Ti_3O_6(OH)_2 + H_2O$	72.84-77.07	16.21-17.15	5.48-5.8	5.47-0
B3	$Fe_{1/2}Ti_3O_{5.5}(OH)_{2.5} + 0.5H_2O$	77-79.35	12.83-13.21	7.23-7.44	2.96-0
B4	$Fe_{1/2}Ti_3O_6(OH)1.5 + H_2O$	77-81.78	12.83-13.62	4.33-4.6	5.78-0
B5	$Fe_{1/3}Ti_3O_6(OH) + H_2O$	81.74-87.06	9.09-9.67	3.09-3.29	6.14-0
B6	$Fe_{1/3}Ti_3O_{5.5}(OH)_2 + 0.5H_2O$	81.74-84.3	9.09-9.36	6.15-6.34	3.05-0
C1	$Fe_{1/2}Ti_3O_5(OH)_{3.5} + 0.5H_2O$	74.88-77.05	12.47-12.83	9.84-10.13	2.81-0
C2	$Fe_{1/2}Ti_3O_{5.5}(OH)_{2.5} + H_2O$	74.88-79.37	12.47-13.22	7.03-7.45	5.62-0
C3	$Fe_{1/2}Ti_3O_6(OH)_{1.5} + 1.5H_2O$	74.88-81.77	12.47-13.62	4.22-4.61	8.43-0
C4	$Fe_{1/3}Ti_3O_{4.5}(OH)_4 + 0.5H_2O$	77-79.31	8.54-8.8	11.58-11.93	2.89-0
C5	$Fe_{1/3}Ti_3O_5(OH)_3 + H_2O$	77-81.7	8.54-9.06	8.68-9.21	5.78-0
C6	$Fe_{1/3}Ti_3O_{5.5}(OH)_2 + 1.5H_2O$	77-84.32	8.54-9.35	5.79-6.34	8.67-0
C7	$Fe_{1/3}Ti_3O_6(OH) + 2H_2O$	77-87.09	8.54-9.66	2.89-3.27	11.56-0
C8	$Fe_{1/3}Ti_3O_5(OH)_3 + 0.5H_2O$	79.3-81.7	8.8-9.08	8.93-9.21	2.98-0
C9	$Fe_{1/3}Ti_3O_{5.5}(OH)_2 + H_2O$	79.3-84.31	8.8-9.35	5.96-6.34	5.95-0
C10	$Fe_{1/3}Ti_3O_6(OH) + 1.5H_2O$	79.3-87.09	8.8-9.67	3-3.28	8.9-0

Furthermore, the hydrated phase proposed in [43] does not conform to the PSR formula $Fe^{3+}_2Ti_3O_9$ [10]. Multiplying the equation of [43] by 1.5 or 3, the obtained phase is well accepted as it extended the LPSR phase as follows:

$$2(Fe^{2+}TiO_3) + H^+$$
$$= Fe^{3+}Ti_2O_5(OH) + Fe^{2+} + e^- \qquad (12)$$
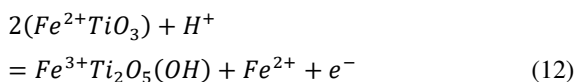
Then, by multiplying by 1.5:

$$3(Fe^{2+}TiO_3) + 1.5H^+$$
$$= Fe^{3+}_{1.5}Ti_3O_{7.5}(OH)_{1.5}) + 1.5Fe^{2+} + 1.5e^- \qquad (13)$$
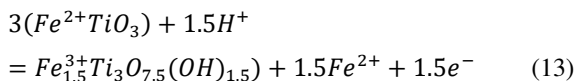
The equation in [43] is considered a definitive extended LPSR phase due to the alteration of ilmenite. According to the prevailing surrounding environmental conditions, if the separated Ti-bearing phase is formed as a micro- or crypto-crystalline randomly distributed phase with the remaining LPSR, the structure will be weakened and collapsed, giving what is called leucoxene. This process can occur in any early stage of the LPSR phases, followed by the LPSR phase of $FeTi_3O_6(OH)_3$. According to [33, 44], after the breakdown of PSR $Fe_2Ti_3O_9$, rutile is developed as oriented aggregates by epitaxial growth in the hexagonal close-packed anion layers of ilmenite. Therefore, rutile is present in a triply twinned

arrangement in altered ilmenite [33, 44]. Then, if the separated Ti-bearing phase is crystallized in the triply twinned rutile phase structure, which seems to have the same XRD pattern as PSR, with the survived remaining LPSR and upon the hexagonal close-packed anion layers of the PSR structure, it will support the structure, and the HPSR can be formed with various successive chemical formula structures.

V.   CONCLUSIONS

This study concluded and illustrated a well-defined new approach to the alteration of ilmenite and the formation of several LPSR phases. The $Fe^{3+}_2Ti_3O_9$ PSR formula phase is relatively more stable than other PSR and LPSR phases. Although the $Fe^{3+}Ti_3O_6(OH)_3$ LPSR phase is unstable, it is considered the most stable lowest iron LPSR phase. When the LPSR formula reaches $FeTi_3O_6(OH)_3$, having almost 69% TiO_2 content, the PSR structure starts to lose some of its structural water, but at a very slow rate. Losing additional Fe^{3+} content from this PSR structure, the number of O^{2-} decreases to less than 6, while the number of OH^- increases above 3. The structure of the obtained LPSR phase becomes somewhat unstable but does not break down suddenly. When the number of O^{2-} becomes much lower than 6, the loss rate of structural water becomes rapid by removing the definite contents of Ti-

and/or Fe- oxyhydroxide phases. The balance between the removal of additional Fe^{3+} from the LPSR formula $FeTi_3O_6(OH)_3$ and the loss rate of structural water may be governed by the prevailing physical conditions of the surrounding environment, especially the activity of water. When approaching the formula $Fe_{0.5}Ti_3O_{4.5}(OH)_{4.5}$, at least 1.5 water molecules, associated with a definite Ti-phase, are removed from the structure of the PSR. At these conditions, the structure of the LPSR formula becomes highly unstable, collapses, and the constituent atoms, especially the most abundant Ti atoms, start to rearrange and recrystallize into a more stable form, most probably rutile.

During the proceeding of the last explained mechanism, three scenarios were obtained. Each of them includes several obtained cases of different molecular formulas for LPSR. A total of 20 cases were obtained. In each case, the content of the separated individual Ti-oxide or Ti-oxyhydroxide phase corresponds to three folds the partially leached LPSR phase content. A careful investigation of the final products obtained from the 20 cases reflects the similarities between some of them. As only the associated individual molecular water content is different, only 10 alteration cases were considered. The chosen 10 cases are suspected to occur only where the unstable immobile titanium oxyhydroxide separated from the LPSR phase after the removal of the first definite iron content. In the chosen ten cases, the true ratio of Ti/(Ti+Fe), which corresponds only to the Ti and Fe contents in the actual remaining LPSR component phase, is 0.75, which is the same as the most stable lowest iron LPSR phase $FeTi_3O_6(OH)_3$. The false ratios that correspond to the total contents of Ti and Fe for all included phases contained within the alteration product for the remaining LPSR and the individual phases of Ti-oxide or Ti-oxyhydroxide are different, as their values range between 0.78 and 0.90.

Two cases of the chosen 10 are similar to the two suggested HPR formulas in [11]. Type II ilmenite alteration, in which ilmenite directly alters to HPR, was considered one of the mixed phases obtained from LPSR and the individual Ti-oxyhydroxide phase. This is an extended alteration process of the $FeTi_3O_6(OH)_3$ LPSR phase, due to iron leaching and hydrolysis processes followed by a separation process for the definite contents of Ti-oxyhydroxides to maintain the survived LPSR structure. When the separated Ti-bearing phase crystallizes in the triply twinned rutile phase structure, it appears to have the same XRD pattern of PSR or HPSR, in association with the survived remaining LPSR upon the hexagonal close-packed anion layers of the PSR structure. This justifies why the structure and the analyzed spot provide the XRD pattern of PSR or HPR. When the alteration rate of PSR is too fast, the successive gradual change will stop at any point between $Fe^{3+}_2Ti_3O_9$ and $Fe^{3+}Ti_3O_6(OH)_3$, or between $Fe^{3+}Ti_3O_6(OH)_3$ and $Fe_{0.5}Ti_3O_{4.5}(OH)_{4.5}$, or at slightly lower iron content, and the structure of PSR/LPSR will collapse. According to the crystallinity of the obtained products, micro- or crypto-individual Ti- and Fe- phases, the detected XRD patterns are governed.

In summary, ilmenite alteration is characterized by the oxidation of Fe^{2+} to Fe^{3+} followed by a continuous loss of Fe^{3+}

to form leached ilmenite and then PSR. This is a near-surface oxidizing process in a slightly acidic environment. The new approach presented in this study is that, on continuous iron leaching and approaching the LPSR phase $FeTi_3O_6(OH)_3$, not only is iron separated, but also Ti-oxy-hydroxides are separated to form individual TiO_2 phases in association with the remaining LPSR phase. At a definite LPSR phase, the structure will break out into individual Ti- and Fe- bearing phases. Furthermore, in this study, the lower stability limit was lower than previously given [9, 28, 33], as it was around 0.5 mol% Fe or slightly lower, related to 3 mol% Ti. At any stage of the last alteration model, and according to changes in environmental conditions, especially acidity and water activity, the occurring LPSR phase can be completely broken out, giving leucoxene with Ti- and Fe- phases with or without identified crystallinity.

ACKNOWLEDGEMENTS

REFERENCES

[1] N. P. Subrahmanyam, N. K. Rao, D. Narasimhan, G. V. U. Rao, N. K. Jaggi, and K. R. P. M. Rao, "Alteration of Beach Sand Ilmenite from Manavalakurichi, Tamil Nadu, India," *Geological Society of India*, vol. 23, no. 4, pp. 168–174, Apr. 1982.

[2] C. Palmer, "Arizonite, ferric metatitanate," *American Journal of Science*, vol. s4-28, no. 166, pp. 353–356, Oct. 1909, https://doi.org/10.2475/ajs.s4-28.166.353.

[3] S. W. Bailey, R. J. Weege, E. N. Cameron, and H. R. Spedden, "The alteration of ilmenite in beach sands," *Economic Geology*, vol. 51, no. 3, pp. 263–279, May 1956, https://doi.org/10.2113/gsecongeo.51.3.263.

[4] A. D. Bykov, "Proarizonite as a secondary mineral due to supergene alteration of ilmenite," in *Proceedings of the USSR Academy of Sciences*, 1964, vol. 156, no. 3, pp. 567–70.

[5] A. K. Temple, "Alteration of ilmenite," *Economic Geology*, vol. 61, no. 4, pp. 695–714, Jun. 1966, https://doi.org/10.2113/gsecongeo.61.4.695.

[6] J. W. Gruner, "The decomposition of ilmenite; discussion," *Economic Geology*, vol. 54, no. 7, pp. 1315–1316, Nov. 1959, https://doi.org/10.2113/gsecongeo.54.7.1315.

[7] D. Carroll, "Ilmenite alteration under reducing conditions in unconsolidated sediments," *Economic Geology*, vol. 55, no. 3, pp. 618–619, May 1960, https://doi.org/10.2113/gsecongeo.55.3.618.

[8] F. Dimanche and D. Bartholome, "The alteration of ilmenite in sediments," *Minerals Science Engineering*, vol. 8, pp. 187–201, 1976.

[9] A. Mücke and J. N. Bhadra Chaudhuri, "The continuous alteration of ilmenite through pseudorutile to leucoxene," *Ore Geology Reviews*, vol. 6, no. 1, pp. 25–44, Feb. 1991, https://doi.org/10.1016/0169-1368(91)90030-B.

[10] M. I. Pownceby, "Alteration and associated impurity element enrichment in detrital ilmenites from the Murray Basin, southeast Australia: a product of multistage alteration," *Australian Journal of Earth Sciences*, vol. 57, no. 2, pp. 243–258, Mar. 2010, https://doi.org/10.1080/08120090903521705.

[11] I. E. Grey and C. Li, "Hydroxylian pseudorutile derived from picroilmenite in the Murray Basin, southeastern Australia," *Mineralogical Magazine*, vol. 67, no. 4, pp. 733–747, Aug. 2003, https://doi.org/10.1180/0026461036740130.

[12] C. C. Gonçalves and P. F. A. Braga, "Heavy Mineral Sands in Brazil: Deposits, Characteristics, and Extraction Potential of Selected Areas," *Minerals*, vol. 9, no. 3, Mar. 2019, Art. no. 176, https://doi.org/10.3390/min9030176.

[13] A. Putnis and C. V. Putnis, "The mechanism of reequilibration of solids in the presence of a fluid phase," *Journal of Solid State Chemistry*, vol. 180, no. 5, pp. 1783–1786, May 2007, https://doi.org/10.1016/j.jssc.2007.03.023.

[14] R. Weibel and H. Friis, "Chapter 10 Alteration of Opaque Heavy Minerals as a Reflection of the Geochemical Conditions in Depositional and Diagenetic Environments," in *Developments in Sedimentology*, vol. 58, M. A. Mange and D. T. Wright, Eds. Elsevier, 2007, pp. 277–303.

[15] M. Dieye, M. M. Thiam, A. Geneyton, and M. Gueye, "Monazite Recovery by Magnetic and Gravity Separation of Medium Grade Zircon Concentrate from Senegalese Heavy Mineral Sands Deposit," *Journal of Minerals and Materials Characterization and Engineering*, vol. 09, no. 06, pp. 590–608, 2021, https://doi.org/10.4236/jmmce.2021.96038.

[16] M. I. Moustafa, "Mineralogy and beneficiation of some economic minerals in the Egyptian black sands," Ph.D. dissertation, Mansoura University, Dakahlia, Egypt, 2010.

[17] N. Z. Boctor, "Mineralogical study of the opaque minerals in Rosetta-Damietta black sands," MSc Thesis, Cairo University, Cairo, Egypt, 1966.

[18] M. A. Mikhail, "Distribution and sedimentation of ilmenite in black sands, west of Rosetta," Ph.D. dissertation, Cairo University, Cairo, Egypt, 1971.

[19] N. M. Hammoud, "Concentration of monazite from Egyptian black sands, employing industrial techniques," MSc Thesis, Cairo University, Cairo, Egypt, 1966.

[20] N. M. Hammoud, "Physical and chemical properties of some Egyptian beach economic minerals in relation to their concentration problems," Ph.D. dissertation, Cairo University, Cairo, Egypt, 1973.

[21] A. A. M. Abdel-Karim, M. I. Moustafa, A. H. El-Afandy, and M. G. Barakat, "Mineralogy, Chemical Characteristics and Upgrading of Beach Ilmenite of the Top Meter of Black Sand Deposits of the Kafr Al-Sheikh Governorate, Northern Egypt," *Acta Geologica Sinica - English Edition*, vol. 91, no. 4, pp. 1326–1338, 2017, https://doi.org/10.1111/1755-6724.13364.

[22] A. A. M. Abdel-Karim, S. M. Zaid, M. I. Moustafa, and M. G. Barakat, "Mineralogy, chemistry and radioactivity of the heavy minerals in the black sands, along the northern coast of Egypt," *Journal of African Earth Sciences*, vol. 123, pp. 10–20, Nov. 2016, https://doi.org/10.1016/j.jafrearsci.2016.07.005.

[23] M. I. Moustafa, "Some Mineralogical Characteristics of the Egyptian Black Sand Beach Ilmenite Part I: Homogeneous Ilmenite and Titanhematite-Ferriilmenite Grains," *Engineering, Technology & Applied Science Research*, vol. 12, no. 6, pp. 9614–9631, Dec. 2022, https://doi.org/10.48084/etasr.5296.

[24] M. I. Moustafa, "Some Mineralogical Characteristics of the Egyptian Black Sand Beach Ilmenite Part II: Rutile-Ilmenite and the Various Titanhematite Grains," *Engineering, Technology & Applied Science Research*, vol. 12, no. 6, pp. 9640–9653, Dec. 2022, https://doi.org/10.48084/etasr.5297.

[25] M. I. Moustafa, "The Mineralogical and Chemical Composition of the Strongly Magnetic Egyptian Black Sand Altered Ilmenite," *Engineering, Technology & Applied Science Research*, vol. 13, no. 4, pp. 11298–11317, Aug. 2023, https://doi.org/10.48084/etasr.6025.

[26] M. I. Moustafa, "Study of the Mineralogical and Chemical Compositions of the Weakly Magnetic Fractions of the Egyptian Black Sand Altered Ilmenite," *Geosciences*, vol. 13, no. 6, Jun. 2023, Art. no. 170, https://doi.org/10.3390/geosciences13060170.

[27] M. I. Moustafa, M. A. Tashkandi, and A. M. El-Sherif, "Detecting Mineral Resources and Suggesting a Physical Concentration Flowsheet for Economic Minerals at the Northern Border Region of Saudi Arabia," *Engineering, Technology & Applied Science Research*, vol. 12, no. 3, pp. 8617–8627, Jun. 2022, https://doi.org/10.48084/etasr.4894.

[28] M. T. Frost, I. E. Grey, I. R. Harrowfield, and K. Mason, "The dependence of alumina and silica contents on the extent of alteration of weathered ilmenites from Western Australia," *Mineralogical Magazine*, vol. 47, no. 343, pp. 201–208, Jun. 1983, https://doi.org/10.1180/minmag.1983.047.343.10.

[29] S. S. Ahmed, M. Y. Miah, C. Qumruzzaman, M. N. Zaman, A. B. Alam, and P. K. Biswas, "Alteration and Exsolution Characteristics of Ilmenites of Moheskhali Island, Chittagong, Bangladesh," *Bangladesh Journal of Scientific and Industrial Research*, vol. 45, no. 1, pp. 17–26, Jan. 1970, https://doi.org/10.3329/bjsir.v45i1.5173.

[30] J. W. Gruner, "Hydrothermal oxidation and leaching experiments; their bearing on the origin of Lake Superior hematite-limonite ores," *Economic Geology*, vol. 25, no. 7, pp. 697–719, Nov. 1930, https://doi.org/10.2113/gsecongeo.25.7.697.

[31] J. W. Gruner, "Hydrothermal oxidation and leaching experiments; their bearing on the origin of Lake Superior hematite-limonite ores; Part II," *Economic Geology*, vol. 25, no. 8, pp. 837–867, Dec. 1930, https://doi.org/10.2113/gsecongeo.25.8.837.

[32] P. A. Schroeder, J. J. Le Golvan, and M. F. Roden, "Weathering of ilmenite from granite and chlorite schist in the Georgia Piedmont," *American Mineralogist*, vol. 87, no. 11–12, pp. 1616–1625, Nov. 2002, https://doi.org/10.2138/am-2002-11-1211.

[33] I. E. Grey and A. F. Reid, "The structure of pseudorutile and its role in the natural alteration of ilmenite," *American Mineralogist*, vol. 60, no. 9–10, pp. 898–906, Oct. 1975.

[34] N. S. Hammoud, "Electrical separation in upgrading Egyptian beach zircon and rutile concentrates," presented at the XIIth International Mineral Processing Congress, Sao Paolo, Brazil, 1977, pp. 100–124.

[35] M. G. Dyadchenko and A. Y. Khatuntseva, "Mineralogy and geochemistry of the weathering process in ilmenite," *Doklady Akademii Nauk SSR, Earth Sciences*, vol. 132, pp. 593–597, 1960.

[36] E. F. Lener, "Mineral Chemistry of Heavy Minerals in the Old Hickory Deposit, Sussex and Dinwiddie Counties, Virginia," MSc Thesis, Virginia Polytechnic Institute and State University, Blacksburg, VA, USA, 1997.

[37] V. Gevorkyan, "Some data on the initial stages of leucoxenization of ilmenite from the sedimentary deposits of the northern Azov area," *Dopovidi Akademi Nauk Ukrains Koi RSR*, vol. 10, pp. 1366–1369, 1964.

[38] G. Pe-Piper, D. J. W. Piper, and L. Dolansky, "Alteration of Ilmenite in the Cretaceous Sandstones of Nova Scotia, Southeastern Canada," *Clays and Clay Minerals*, vol. 53, no. 5, pp. 490–510, Oct. 2005, https://doi.org/10.1346/CCMN.2005.0530506.

[39] S. Tetsopgang, J. Koyanagi, M. Enami, and K. Kihara, "Hydroxylian pseudorutile in an adamellite from the Nkambe area, Cameroon," *Mineralogical Magazine*, vol. 67, no. 3, pp. 509–516, Jun. 2003, https://doi.org/10.1180/0026461036730113.

[40] A. Derkowski and A. Kuligiewicz, "Rehydroxylation in smectites and other clay minerals observed in-situ with a modified thermogravimetric system," *Applied Clay Science*, vol. 136, pp. 219–229, Feb. 2017, https://doi.org/10.1016/j.clay.2016.11.030.

[41] V. A. Drits, A. Derkowski, and D. K. McCarty, "New insight into the structural transformation of partially dehydroxylated pyrophyllite," *American Mineralogist*, vol. 96, no. 1, pp. 153–171, Jan. 2011, https://doi.org/10.2138/am.2011.3605.

[42] V. A. Drits, A. Derkowski, and D. K. McCarty, "Kinetics of partial dehydroxylation in dioctahedral 2:1 layer clay minerals," *American Mineralogist*, vol. 97, no. 5–6, pp. 930–950, May 2012, https://doi.org/10.2138/am.2012.3971.

[43] V. D. Ignatiev, "Solid-phase mechanism of the ilmenite leucoxenization," *Lithology and Mineral Resources*, vol. 34, pp. 184–189, 1999.

[44] G. Teufer and A. K. Temple, "Pseudorutile—a New Mineral Intermediate between Ilmenite and Rutile in the N Alteration of Ilmenite," *Nature*, vol. 211, no. 5045, pp. 179–181, Jul. 1966, https://doi.org/10.1038/211179b0.